Morphology Development in Thin Films of a Lamellar Block Copolymer Deposited by Electrospray

ARTICLE *in* MACROMOLECULES · AUGUST 2014

Impact Factor: 5.8 · DOI: 10.1021/ma500376n

3 AUTHORS, INCLUDING:

Hanqiong Hu
Yale University
12 PUBLICATIONS **88** CITATIONS
SEE PROFILE

Jonathan Phillip Singer
Rutgers, The State University of New Jersey
26 PUBLICATIONS **536** CITATIONS
SEE PROFILE

Macromolecules

Article

pubs.acs.org/Macromolecules

Morphology Development in Thin Films of a Lamellar Block Copolymer Deposited by Electrospray

Hanqiong Hu,[†] Jonathan P. Singer,[†] and Chinedum O. Osuji*,[†]

[†]Department of Chemical Engineering, Yale University, New Haven, Connecticut 06511, United States

Supporting Information

ABSTRACT: Electrospray has been recently advanced as a novel approach for the continuous deposition of self-assembled block copolymer thin films. It represents an analogue of physical vapor deposition in which the development of well-ordered microstructures is predicated on relatively rapid relaxation of the polymer compared to its rate of deposition. Here we describe the morphology development of a lamellae-forming poly(styrene-*b*-4-vinylpyridine) deposited by electrospray. Morphology was considered in the context of relative changes of the deposition and relaxation rates, with the latter significantly affected in some cases by the presence of residual solvent. We observe that the presence of residual solvent in deposited material accelerates the equilibration kinetics such that well-ordered alternating lamellar morphologies could be produced at deposition rates as high as 55 nm/min under "wet" spray conditions, whereas hexagonally packed micelles were produced when the polymer was deposited free of solvent, denoted as the "dry" spray limit. Molecular weight (MW) plays an important role in equilibration kinetics in the "dry" limit with a transition from poorly ordered to well-ordered lamellae produced by reducing MW. Film morphology was largely insensitive to temperature and flow rate over a broad range from 150 to 210 °C and from 3 to 18 μL/min respectively, although the orientation of the lamellae switched from parallel to perpendicular at elevated flow rates, potentially due to the influence of rapid solvent evaporation.

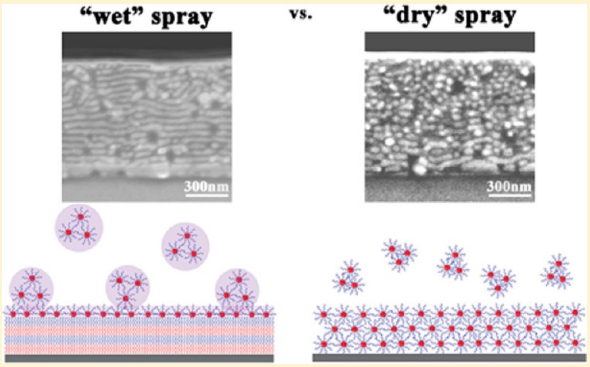

INTRODUCTION

Block copolymers (BCPs) are promising nanostructured materials that undergo microphase separation and self-assemble into periodic nanostructures with characteristic length scales from ca. 3 to 100 nm. The ease of tuning nanostructure based on molecular composition and architecture makes BCPs attractive materials for nanotechnology applications, such as masks for pattern transfer,[1−3] templates for nanomaterials synthesis,[4−6] photonic crystals,[7−9] separation and fuel cell membranes,[10−13] and heterojunction photovoltaics.[14,15] The provision of adequate microstructural control is essential for producing the near-defect-free morphologies, which are desired in the above-mentioned areas, as recently reviewed.[16] Achieving long-range order in the BCP morphology is often accomplished by postdeposition annealing processes. Thermal annealing can be used to produce equilibrium situations in which morphology is a function of the particular interfacial wetting conditions[17] and thickness commensurability. Recent work by Bates et al. sheds new light on this.[18] By contrast, solvent vapor annealing can provide access to nonequilibrium configurations that are kinetically locked-in on the removal of the plasticizing vapor.[19−21] External fields, such as shear,[22,23] electric fields,[6,24] and magnetic fields,[25,26] provide the ability to control the orientation of the microstructure while also improving long-range order to some degree as well. With notable exceptions,[27,28] external fields are usually not viable approaches for controlling structure in thin films, i.e., where thickness is less than ca. 1 μm.

The prototypical approach to BCP thin film processing involves deposition by spin-coating and the use of thermal or solvent vapor annealing to control the development of the system morphology. Generally speaking, this does not provide control for films beyond 1 μm in thickness, and deposition occurs in a single step as opposed to in the continuous fashion that is better suited to roll-to-roll operations. The recently developed zone annealing approach[29−31] is attractive for scalable thin film processing, as it enables fabrication of ordered structures over large areas on flexible substrates and is compatible with roll-to-roll technology.[32] In zone annealing, the film morphology can be controlled by adjusting the magnitude of the temperature gradient in the thermal zone and further enhanced by combination of soft shear.[33] Another technique, zone-casting, was recently advanced by Tang et al. as a robust unidirectional solution casting method that slowly deposits block copolymer solution onto a moving substrate from a nozzle held perpendicular to the direction of

Received: February 19, 2014
Revised: July 7, 2014
Published: August 13, 2014

motion.[34,35] Diverse morphologies with excellent orientational and lateral order can be cast by controlling solution casting rates, temperatures, etc., and are independent of the substrates.

While both zone-annealing and zone-casting are excellent examples of continuous processing with the capability of directing self-assembly over large areas, the resulting film morphologies are nonequilibrium structures that are kinetically trapped. Electrospray deposition represents an alternative for continuously depositing ordered block copolymer films with the ability to tune the deposition conditions to render either thermally equilibrated or kinetically trapped (solvent-dictated) morphologies.[36] This process enables the deposition of equilibrated morphologies in a continuous fashion through the production and deposition of submicrometer droplets of dilute BCP solutions under high electrical voltage. The size of droplets produced in the cone-jet mode of deposition, D, is well described by eq 1,[37] where α is a constant related to the fluid's dielectric permittivity, Q is the flow rate, ε is the dielectric constant, ρ_s is the fluid density, γ is the surface tension, and σ is the conductivity of the liquid. The number of chains in an arriving droplet (n_c) is a simple function of the droplet diameter in μm (D), the concentration of the feed solution expressed in terms of polymer volume fraction (ϕ), the polymer mass density in g/cm^3 (ρ), the molecular weight of the polymer in g/mol (MW), and Avogadro's constant (N_A) (eq 2).

$$D = \alpha\left[\frac{Q^3\varepsilon\rho_s}{\pi^4\sigma\gamma}\right]^{1/6} \tag{1}$$

$$n_c = 10^{-12}\left[\frac{\pi D^3}{6}\varphi\rho\frac{N_A}{MW}\right] \tag{2}$$

In this process, no more than ca. 0.1 fg of polymer (a mass of diameter ca. 50 nm or roughly 300 chains of MW = 100 kg/mol for ϕ = 0.01 vol %, ρ = 1 g/cm^3) is deposited in discrete droplets onto a heated substrate, with the carrier solvent evaporating during the electrospray transport. Relaxation of the deposited material is accelerated by heating the substrate such that thermally equilibrated morphologies can be produced. Our previous study[36] demonstrated the preservation of the substrate-directed vertical orientation in a cylinder-forming PS-*b*-PMMA system on a neutral substrate indicated by the continuity of domains over 500 nm in thickness. Parametric studies on a cylinder-forming PS-*b*-PEO system also revealed that perpendicular orientation could be produced on a preferential substrate by modifying the preference of solvent-mediated interface and that surface morphology was dependent on various spray parameters, such as solvent selection, substrate temperature, and feed solution flow rate.

There is a large parameter space to explore in BCP electrospray deposition, and there is currently little knowledge surrounding the topics of equilibration kinetics and structure development in these systems. While the strict analogy to physical vapor deposition envisions equilibration of deposited material as a result of thermal annealing only, the potential presence of residual solvent in deposited material or solvent vapor in the near vicinity provides extra degrees of freedom in tuning the equilibration kinetics by solvent accelerated or solvent vapor annealing, respectively. The residual solvent at deposition can assist the wetting and relaxation of the polymer as a plasticizer, and further, the directional field generated by rapid evaporation at the heated interface can also influence the orientational order of the deposited film.[19] In this study we examine the structural development of a lamellar poly(styrene-*b*-4-vinylpyridine) (PS-*b*-P4VP) thin film produced by electrospray deposition. We explore the effect of particle dryness, deposition temperature, and solvent composition on the equilibration kinetics and final morphology of the deposited films. Particle dryness, or the amount of residual solvent in deposited material, is determined collectively by the original droplet size and its flight time to the substrate during which evaporation takes place. For a given droplet size, flight time is principally a function of the distance between the electrospray needle and the substrate (the collection distance), the electrospray voltage (which produces an electric field that accelerates droplets to the substrate), and the temperature experienced by the droplet during flight, which in the near-substrate region is a function of the substrate temperature. Equilibrated parallel layers can be deposited using a wide range of spray parameters as a result of balanced thermal and residual solvent annealing. As the amount of residual solvent is reduced by increasing the separation between the electrospray needle and the substrate, the film morphology transitions into hexagonally packed micelles due to insufficient relaxation in the "dry" spray limit. Favorable equilibration kinetics under thermal annealing alone in the dry spray limit can be restored, however, by using lower molecular weight polymers. These findings provide important insights into the dynamics of structure evolution during electrospray deposition of BCPs.

EXPERIMENTAL SECTION

Two lamellae-forming PS-*b*-P4VP were purchased from Polymer Source, Inc. with molecular weights of PS/P4VP 20/17 and 5/5 kg/mol, respectively. All solvents were used as received (Sigma-Aldrich Corp.). Electrospray deposition of PS-*b*-P4VP thin films was conducted in the cone-jet mode as previously described[36] and illustrated in Figure 1. Dilute solutions ranging in composition from

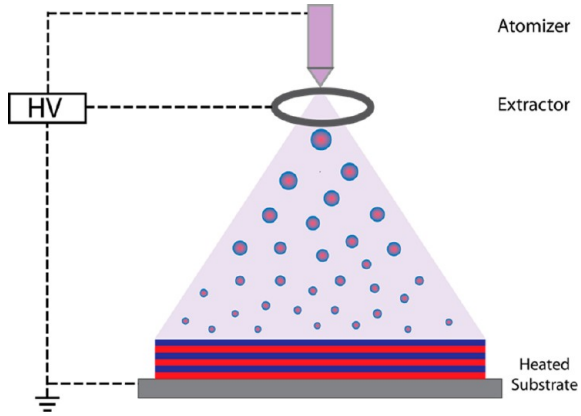

Figure 1. Schematic of BCP electrospray deposition.

0.01 to 0.3 wt % PS-*b*-P4VP in various solvent mixtures were fed into the needle, which acted as a liquid atomizer, using a programmable syringe pump at flow rates from 3 to 27 μL/min. The solution became charged under the influence of high voltage and broke into fine droplets, the sizes of which have been previously shown to follow the scaling law of eq 1.[36] The droplets were collected on silicon substrates placed on a temperature-controlled electrically grounded plate at prescribed temperatures between 135 and 210 °C at distances between 3 and 9 cm from the needle tip. Substrates were thereafter cleaved under liquid nitrogen to expose the edges of the film for cross-sectional SEM imaging of the BCP morphology (Hitachi SU-70 SEM, 2 kV accelerating voltage). Surface morphology was not characterized,

dx.doi.org/10.1021/ma500376n | Macromolecules 2014, 47, 5703−5710

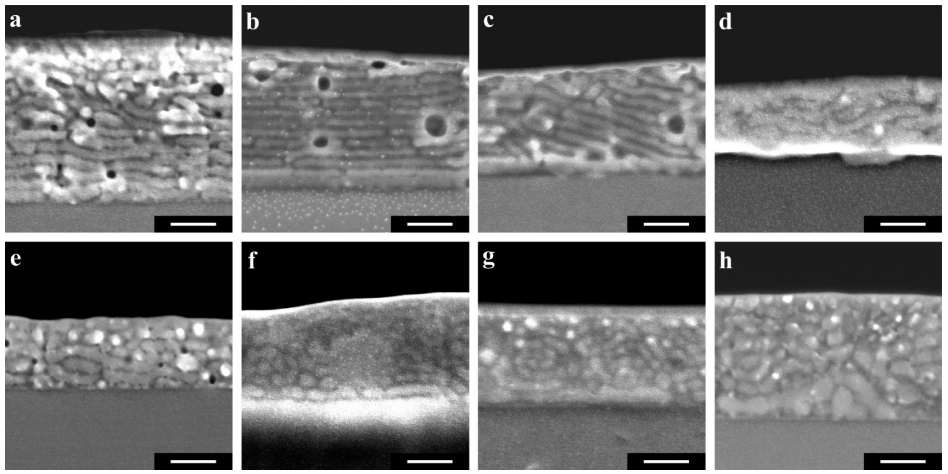

Figure 2. Cross-sectional SEM images of PS-*b*-P4VP (20K−17K) film sprayed from 0.03 wt % solutions of pure and mixed solvents onto substrate at 195 °C and 5 cm collection distance. Solubility parameters of the solvents increase from 18.7 to 24.7 $MPa^{1/2}$. For the mixed solvents A/B, the majority component A is present at 80 vol %. (a) THF/acetone, (b) chloroform/acetone, (c) MEK, (d) toluene/ethanol, (e) THF/ethanol, (f) chloroform/ethanol, (g) acetone/ethanol, and (h) DMF solutions. Scale bar: 200 nm.

Table 1. Summary of Relative Dielectric Constants (ε_r) at 20 °C, Boiling Points (bp), Vapor Pressure (vp) at 20 °C, and Hildebrand Solubility Parameters (δ) of Solvents Used in the Work[a]

	PS	P4VP	chloroform	acetone	THF	ethanol	toluene	MEK	DMF
T_g (°C)	105	140							
ε_r			4.81	20.7	7.58	24.5	2.38	18.51	36.7
bp (°C)			61	56	66	78	110	80	153
vp (Torr)			158.4	184.5	142	43.9	28.5	74	2.7
δ ($MPa^{1/2}$)	18.6	23	18.7	19.7	18.5	26.2	18.3	19.3	24.7

[a]Data are assembled from various sources.[38−40]

as the preferential wetting condition meant that the lamellar morphology was blurred by a wetting layer at the free surface (Supporting Information, Figure S1). Samples were stained with iodine at room temperature, which selectively associates with P4VP, rendering it bright under SEM. Where needed, and particularly for the lower MW system (5K−5K), images were contrast-enhanced digitally for ease of viewing. Occasional aggregation of iodine during staining appears as large bright spots in SEM imaging. In some cases, cavities were produced during deposition due to entrapment of air and/or the formation of solvent vapor pockets.

RESULTS AND DISCUSSION

1. Solvent Selectivity. PS-*b*-P4VP film morphologies sprayed from different solvent combinations are shown in Figure 2a−h. The properties of solvents used in the study are summarized in Table 1. It can be clearly seen that films sprayed from chloroform/acetone (Figure 2b) exhibit the best ordering in the resulting lamellae, as judged by the clear delineation and persistence of domains. Films sprayed from tetrahydrofuran/acetone (THF/acetone), methyl ethyl ketone (MEK), and toluene/ethanol solutions (Figure 2a,c,d) are less-well-ordered with more defects in the lamellae, while those sprayed from THF/ethanol, chloroform/ethanol, acetone/ethanol, and dimethylformamide (DMF) solutions (Figure 2e−h) display no signs of long-range ordering.

Overall, our results suggest that ordered lamellar morphologies are produced from solvents that are preferential for the PS block, while those that were selective for P4VP led to poorly ordered morphologies. This can be seen for both mixtures and pure solvent systems. For example, the solvent system of chloroform and acetone led to well-ordered lamellae, whereas in the acetone/ethanol system (i.e., with ethanol as the dominant solvent at deposition given the difference in solvent volatility as discussed later) short lamellae and micellelike structures were observed. This also held for the pure solvent systems of MEK and DMF. Mixtures of PS-selective solvents with P4VP-selective solvents yielded morphologies that were intermediate between the well-ordered and poorly ordered structures observed for PS-selective and P4VP-selective systems. The results of Figure 2 suggest that the solubility parameter of the solvent plays a large role in dictating the final structure observed in the deposited films, at a fixed deposition rate, temperature, and collection distance.

We have shown in previous work that solvent selectivity plays an important role in determining surface morphologies of electrosprayed thin films of PS-*b*-PEO through mediation of interfacial preference.[36] The electrical conductivity, volatility, and block selectivity of the solvent can affect the electrospray process itself, as well as the equilibration behavior of the deposited materials. The electrical conductivity of the solvent is an important factor in determining the size of the droplets, with smaller droplets produced by more conductive solvents, as indicated by eq 1. Due to the low electrical conductivities of chloroform, THF, and toluene, small amounts of either acetone or ethanol were added to these solvents as needed to enable stable electrospray in the cone-jet mode. Solvent volatility influences the dryness of the deposited material for a given droplet size due to faster evaporation during droplet flight for more volatile solvents. In our selection of solvents, the conductivity and volatility do not vary much except in the case of DMF, which is more conductive and less volatile than the other solvents used. We find that the solvent selectivity is a

dx.doi.org/10.1021/ma500376n | *Macromolecules* 2014, 47, 5703−5710

Table 2. Summary of Boiling Point Difference (Δbp) and Solubility Parameters of Solvent Mixtures (δ_m) Used in This Work[a]

	chloroform/acetone	THF/acetone	toluene/ethanol	chloroform/ethanol	acetone/ethanol	THF/ethanol
Δbp (°C)	5	10	32	−17	−22	−12
δ_m ($MPa^{1/2}$)	18.9	18.7	19.9	20.2	21.0	20.0

[a]Following common practice, the solubility parameters for solvent mixtures were calculated using a volume weighted linear mixing law.[42]

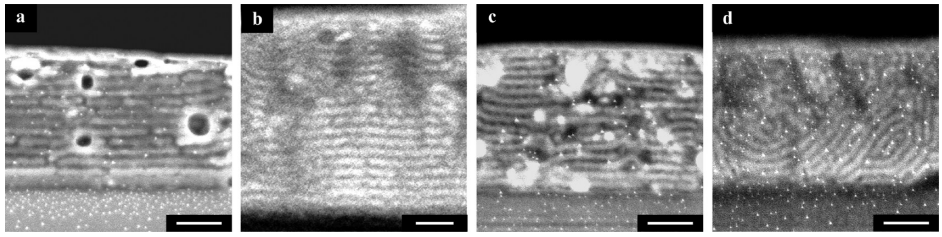

Figure 3. Cross-sectional SEM images of PS-*b*-P4VP (20K−17K) film sprayed from 0.03 wt % chloroform/acetone at (a) 3 μL/min, (b) 9 μL/min, (c) 18 μL/min, and (d) 27 μL/min at 195 °C and 5 cm separation. Scale bar: 200 nm.

stronger determining factor in the film morphology than either volatility or conductivity. The solubility parameter of PS is reported as 18.6 $MPa^{1/2}$,[41] while that of P4VP is around 23 $MPa^{1/2}$.[42] THF is generally considered a good nonselective solvent for the system, while chloroform and toluene are selective for PS, and DMF and ethanol are very selective for P4VP. Since solvent evaporates during droplet transport to the substrate, the solubility parameter of the solvent mixture and thus its selectivity will change if there is a significant difference in the volatility between the solvents, which can be associated with large differences in solvent boiling points. Table 2 summarizes the difference of boiling points between the binary solvent mixtures and the combined solubility parameters. If there is a large difference in the boiling point, especially in more volatile solvent systems, the selectivity is principally determined by the less volatile solvent, such as in the cases of acetone/ethanol and chloroform/ethanol mixtures, where ethanol dominates the selectivity. When both solvents have relatively high boiling points, or similar volatilities, the mixture is presumed to behave in a manner reflecting the effect of a combined or effective solubility parameter.

From the solubility parameters in Table 1, MEK is slightly selective for PS, while DMF is strongly selective for P4VP. The lower volatility of DMF might also contribute to the poor ordering due to disruption of previously deposited material by an excessive quantity of residual solvent at deposition. It is known that block copolymer ordering is favored by the use of solvents with balanced block solvency. We speculate that the strong asymmetry in the degree of selectivity of the PS- vs P4VP-selective solvents is responsible for the differences observed in ordering behavior. That is, the differences between the mean solubility parameter of the BCP and the P4VP-selective solvents are much greater than the corresponding differences for the PS-selective solvents. Additionally, in solvent mixtures involving ethanol, the lower volatility of this highly P4VP-selective solvent (nonsolvent for PS) results in an enhancement of its concentration as the droplets travel to the substrate. To some extent this is an oversimplification, as residual solvent and therefore solvent volatility, as well as solvent vapor annealing, can play nontrivial roles in the assembly of the lamellar structure once the BCP is deposited on the substrate. These factors are discussed below in the sections that follow. On the basis of the well-ordered morphology produced with chloroform/acetone mixtures, this solvent composition was taken as a standard for investigations of other effects.

It is apparent from Figure 2 that the final film thicknesses and therefore the deposition times were not identical across all samples. It should be noted that this, however, does not play a significant role when considering the equilibration of the morphology of the films due to the real-time nature of the deposition process. That is, since the films were not subjected to any postdeposition annealing, the morphology displayed reflects the result of polymer equilibration during deposition only and we could therefore address our concern for the ability of the film to order within the constraints established by the combination of experimental parameters. In all cases, the films displayed morphologies that either represented complete equilibration with the surface (uniformly parallel lamellae) or were sufficiently thick that the dependence of the morphology, as a function of height within the film, reflected the nonequilibrated nature of the system.

2. Feed Solution Flow Rate. We examined the morphology of films deposited under various flow rates using chloroform/acetone solvent mixture. As shown in Figure 3a−c, well-ordered films were produced with parallel lamellae when sprayed at flow rates from 3 to 18 μL/min. Within this range, the film roughness on length scales >10 μm increases with flow rate due to faster deposition (Supporting Information, Figure S2), but the overall quality of ordering locally does not vary much. At the highest flow rate considered, however, 27 μL/min, we observed a nonparallel orientation of ordered lamellae (Figure 3d).

The flow rate of the feed solution affects both the size of the droplet emitted from the nozzle and the overall deposition rate of the film. For electrospray operated in the cone-jet mode as done here, the droplet diameter scales with the square root of the flow rate as shown in eq 1. Locally, the mass of material delivered in a single droplet scales as $Q^{3/2}$. By changing the flow rate from 3 to 27 μL/min, we have effectively increased the size of the droplet by a factor of 3 and the mass of polymers in each droplet by a factor of 27. The average film deposition rate also increases with the flow rate but in a sublinear fashion, as a higher flow rate leads to a small increase in the deposition area. Higher flow rates therefore require faster equilibration kinetics to support the evolution of well-ordered morphologies. Nevertheless, in our earlier work[36] it was observed that higher flow rates not only increased the BCP deposition rate but also

dx.doi.org/10.1021/ma500376n | Macromolecules 2014, 47, 5703−5710

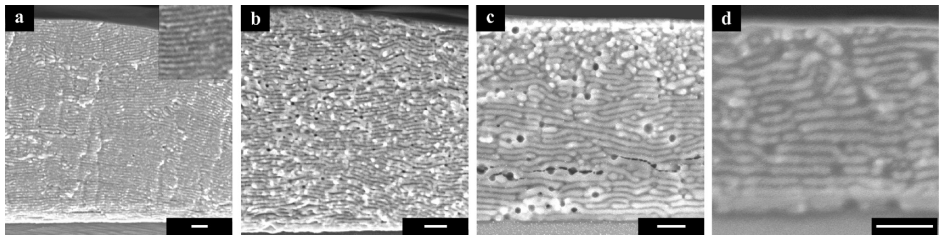

Figure 4. Cross-sectional SEM images of PS-P4VP (20K−17K) film sprayed from (a) 0.3 wt % (inset is the magnification of a 500 nm portion of the film), (b) 0.1 wt %, (c) 0.03 wt %, and (d) 0.01 wt % chloroform/acetone solution at 3 μL/min and 195 °C substrate temperature. Scale bar: 250 nm. Deposition rates are 55, 35, 8, and 2.5 nm/min, respectively.

increased the amount of residual solvent in deposited material due to the larger quantity of solvent in each droplet and the longer flight time required to fully remove this solvent by evaporation. Residual solvent can accelerate the equilibration kinetics of the system by providing the polymer chains added mobility relative to completely dry materials. Additionally, residual solvent can also affect the film morphology by modifying the wetting interaction of the polymer with the substrate. It is likely that a substantial amount of residual solvent is present in at the highest flow rate of 27 μL/min. We speculate that rapid transport of the vaporized solvent through the deposited material leads to a directional ordering field perpendicular to the film surface, thus resulting in more vertically aligned lamellae.

3. Feed Solution Concentration. We considered the effect of feed solution concentration on morphology of films deposited at increasing rates. We found that the film microstructure is surprisingly insensitive to changes in the deposition rate over a wide range, with well-ordered lamellae produced in all cases, as shown in Figure 4. Even with the most concentrated solution of 0.3 wt % used in this study, well-ordered parallel lamellae were achieved for up to a 3.5 μm thick film.

While adjusting the flow rate can change the deposition rate, the resulting difference in the quantity of residual solvent delivered for a fixed collection distance complicates an understanding of this effect. By changing the solution concentration, however, the deposition rate was tuned without varying the amount of solvent in the deposited material where, to first order, the solvent evaporation kinetics during flight is independent of the polymer concentration. This is a reasonable assumption, particularly at the very low concentrations employed here.[43,44] At a fixed flow rate, the deposition rate increases linearly with increasing polymer concentration, assuming the deposition area remains the same. This again is a reasonable assumption, as the dynamics of electrospray atomization are largely unaffected by the small changes in polymer concentration considered here, with all solutions in the dilute limit as we estimate the overlap concentration c^* to be no less than 1.5 wt % based on PS chain statistics in good solvent. This is corroborated by the observed ca. 22 times change in the deposition rate from 2.5 to 55 nm/min on increasing the feed solution concentration 30 times from 0.01 to 0.3 wt %. As discussed earlier, equilibration kinetics is a function of deposition rate, substrate temperature, and residual solvent content. The results here indicate that the deposition temperature, residual solvent content, and collection distance are sufficient to permit effective relaxation of the arriving material and assembly of well-ordered lamellae.

4. Deposition Temperature. The dependence of film morphologies on temperature is summarized in Figure 5. In our

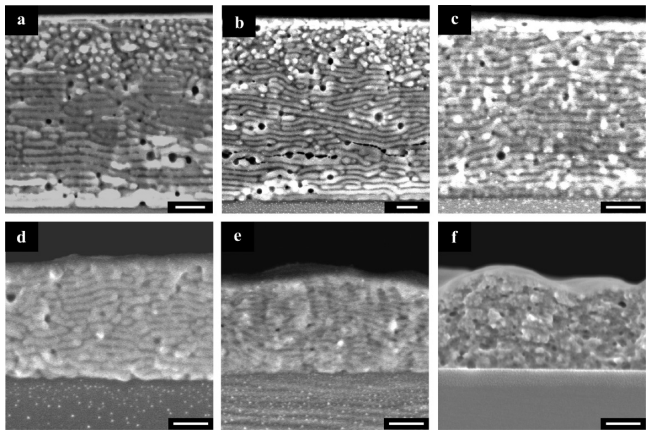

Figure 5. Cross-sectional SEM images of PS-*b*-P4VP (20K−17K) film sprayed from 0.03 wt % chloroform/acetone solutions at (a) 210 °C, (b) 195 °C, (c) 180 °C, (d) 165 °C, (e) 150 °C, and (f) 135 °C. Scale bar: 200 nm.

system, PS has a T_g of 105 °C, while P4VP has a higher T_g of 140 °C. Better lamellar ordering was observed with higher deposition temperatures. Reduction of the deposition temperature resulted in less parallel lamellae, which exhibited more defects relative to lamellae produced at higher deposition temperatures. This indicates that the system is unable to adopt the thermodynamically preferred parallel orientation. At the lowest temperature, which is under the T_g of both blocks, the microstructure of the system was not discernible. Interestingly at very high temperatures (210 °C and also occasionally at 195 °C), what appear to be hexagonally packed spherical micelles were visible in the near surface regions of films, with a transition to well-ordered lamellae deeper into the film.

The inability of the system to display the thermodynamically preferred parallel arrangement of lamellae at lower deposition temperatures is likely due to limited chain mobility at the temperatures considered, relative to the rate of deposition. The absence of discernible microstructure for the lowest deposition temperature is consistent with an inability of the system to relax from the as-deposited chain conformations into well-ordered parallel lamellae. At a given deposition rate, the equilibration kinetics, and thereby the film morphology, is determined by the ability of polymer chains to equilibrate with their surroundings via diffusive motion. The diffusivity of the block copolymer is a strong function of the substrate temperature, and as an activated process is expected to scale with inverse temperature exponentially as $D \sim D_0 \exp[-E_a/kT]$, where E_a is the

dx.doi.org/10.1021/ma500376n | *Macromolecules* 2014, 47, 5703−5710

activation energy for diffusion and T is the absolute temperature. In the absence of the plasticizing effect of residual solvent or ambient solvent vapor, production of equilibrated morphologies requires thermally annealing the deposited material at temperatures well above the nominal glass transition temperatures (T_g) of the constituent blocks to achieve the required chain mobility.

Recent studies have demonstrated the possibility of largely decreasing equilibration time when combining solvent and thermal annealing, such as in the case of solvothermal annealing[45] or microwave heating under solvent-rich atmospheres.[46,47] The role of temperature in electrospray is often convoluted with solvent annealing, unless efforts are made to ensure delivery of completely dry material to the substrate. The substrate temperature therefore not only affects chain diffusion at deposition but also tunes solvent content of the arriving particle and potentially solvent vapor pressure in the immediate vicinity of the film surface.

While the "micelle-to-lamellae" transition will be addressed in greater detail later, we suspect that the morphology at elevated deposition temperatures was a result of reduced residual solvent at deposition due to increased solvent loss from arriving droplets in the near vicinity of the heated substrate, where there is substantial convective heat flow. In fact, these samples represent a snapshot of the crossover between solvent-mediated and thermally mediated annealing, where only some of the ordering occurs in the presence of residual solvent and a majority of the annealing happens through slower (though accelerated by the higher temperature) thermal means.

5. Collection Distance: Needle–Substrate Separation. Decreasing the separation from 5 to 3 cm resulted in films that displayed a similar level of ordering (Figure 6a,b). As shown in Figure 6b–d, film morphology evolved from alternating parallel lamellae to increasingly disordered lamellae and eventually spherical micellelike features when collection distances increased from 5 to 7 to 9 cm, respectively. Films deposited at a collection distance of 9 cm at an even higher temperature of 210 °C retained the same micellelike morphology as at 195 °C (Supporting Information, Figure S3).

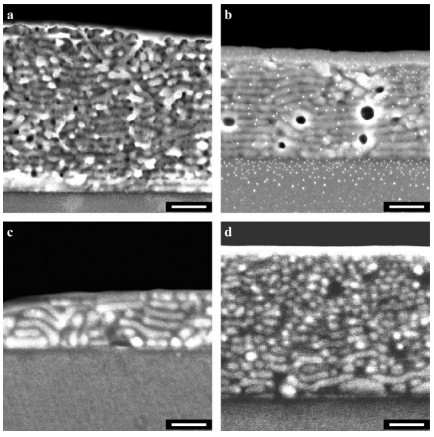

Figure 6. Cross-sectional SEM images of PS-*b*-P4VP (20K–17K) film sprayed from 0.03 wt % chloroform/acetone solutions at 3 μL/min with separations of (a) 3 cm, (b) 5 cm, (c) 7 cm, and (d) 9 cm at 195 °C. Scale bar: 200 nm.

We have described the importance of residual solvent content in modifying the effective equilibration kinetics. One approach to alter the residual solvent content is to adjust the droplet flight time by collection distance. As depicted in Figure 1, droplets undergo evaporation as they travel from the electrospray needle to the substrate and become increasingly polymer rich and solvent poor as a result. Therefore, we expect to collect drier particles at larger needle–substrate separations due to increased droplet flight times. The similarity in morphologies produced at separation distances of 3 and 5 cm suggests that any increase in residual solvent due to this change was negligible in effect. On the other hand, utilization of a sufficiently large collection distance should bring the system into a regime where the accelerated equilibration due to residual solvent is effectively lost for a given flow rate as the deposited material crosses a lower threshold of solvent concentration. This would leave only thermal annealing to affect the final morphology.

The "micelle-to-lamellae" transition as a function of decreasing deposition distance demonstrates unambiguously the role of residual solvent content in determining the equilibration kinetics in the electrospray deposition process. Since PS-*b*-P4VP is a strongly segregated system, we expect micelle formation (or other self-assembly) even in the presence of a good solvent once the polymer concentration within the droplet is above a certain threshold. This is schematically illustrated in Figure 7a. Given the rapid rate of evaporation, it is likely that the system becomes kinetically trapped in this state as it is delivered to the substrate. At large enough collection distances, the solvent evaporates completely, leading to the deposition of solvent-free material, which we denote as the "dry" spray limit. The real-time annealing may be insufficient to permit the PS-*b*-P4VP micelles to relax into the equilibrium lamellar morphology at the prescribed temperature and deposition rate, resulting in the production of hexagonally packed micelle arrays (Figure 7b). At smaller collection distances, material is deposited with more residual solvent, which can accelerate the structural relaxation to lamellae through micelle-fusion by plasticizing the system and potentially also by modifying the wetting behavior of deposited material (Figure 7c). As the deposition continues, alternating lamellae can grow to many layers (Figure 7d).

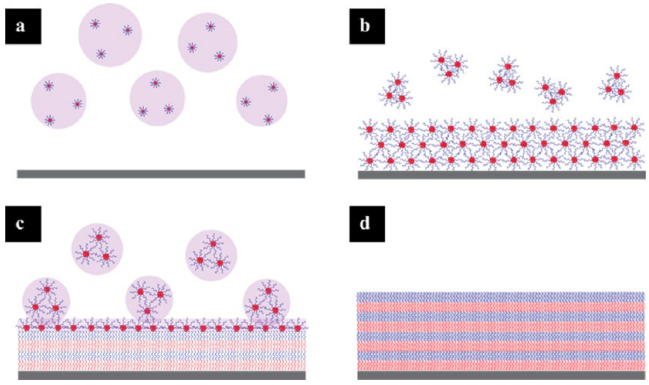

Figure 7. Illustration of self-assembly of PS-*b*-P4VP in the electrospray deposition process. (a) Transport of droplets containing PS-*b*-P4VP micelles to the substrate; (b) solvent completely evaporates at large enough separations, leaving dry micelles that are unable to relax into lamellae; (c) micelles are collected with solvent still present at small/intermediate separations, and residual solvent helps transformation of micelles into lamellae; (d) continuous growth of lamellae under "wet" spray conditions.

dx.doi.org/10.1021/ma500376n | *Macromolecules* 2014, 47, 5703–5710

6. Molecular Weight Dependence. We experimented with a low molecular weight (MW) PS-*b*-P4VP (5K−5K) under standard spray conditions (Figure 8a), lower temperature

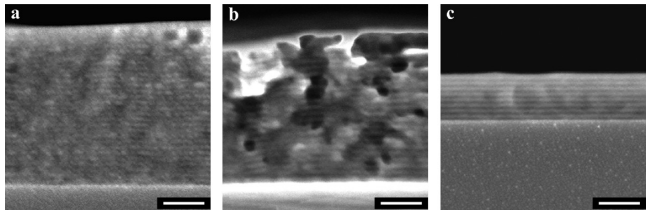

Figure 8. Cross-sectional SEM images of PS-*b*-P4VP (5K−5K) film sprayed from 0.03 wt % chloroform/acetone solution at (a) 5 cm, 195 °C; (b) 5 cm, 150 °C; and (c) 9 cm, 195 °C at 3 μL/min. Scale bar: 100 nm.

spray (Figure 8b), and "dry" spray (Figure 8c). Contrary to the results in the higher MW system, well-ordered lamellae morphologies were achieved under all three conditions and with an even higher degree of order.

The equilibration kinetics in the dry spray limit is presumably dictated solely by the polymer diffusivity, free of any solvent-mediated effects. As such, the 5K−5K material could produce well-ordered lamellae under the conditions that resulted in poorly equilibrated structures for 20K−17K material due to enhanced diffusivity of chains based on unmodified reptation theory, $D \sim MW^{-2}$, for entangled polymer melts.[48] Apart from the molecular weight dependence of the polymer diffusivity, the low molecular weight material used here has block molecular weights that are well below the entanglement molecular weights for PS (M_e^{PS} = 13.3 kg/mol)[49] and P4VP ($M_e^{P4VS} \sim M_e^{PS}$), which provides drastically higher mobility relative to the higher MW system. The ability to produce ordered morphologies under thermal annealing alone represents a useful situation, as one can use this to make fundamental explorations in equilibrium self-assembly of continuously deposited thin films in the presence of various surface features of external stimuli.

CONCLUSION

We have considered here the importance of a range of process parameters on the morphology of lamellar block copolymer thin films produced by electrospray deposition. The microstructure was strongly influenced by the selectivity of the carrier solvent with the degree of ordering improving with the selectivity of the solvent for the PS block. An 80/20 mixture of chloroform/acetone displayed the best ability to produce well-ordered thin films. The morphology was largely insensitive to the flow rate of the feed solution over a broad range from 3 to 18 μL/min, which suggests that residual solvent in deposited material may assist ordering. The transition from parallel to perpendicular orientation at the highest flow rate of 27 μL/min underlines the role of residual solvent in affecting the morphology, in this case presumably through an in situ directional solvent vapor evaporation or annealing effect. Film morphology was found to be insensitive to concentration of the feed solution, with ordered morphology preserved up to a deposition rate of 55 nm/min at relatively low flow rates (3 μL/min) and high substrate temperature (195 °C). The ability of the film to equilibrate over such a wide range of deposition rates again suggests that residual solvent at deposition plays a significant role in ordering. This is highlighted by results obtained when the quantity of residual solvent is decreased by increasing the droplet flight time via the collection distance. In this case, poorly ordered films are obtained that appear to be kinetically trapped micellar domains which are unable to equilibrate in real time with the substrate to produce the equilibrium parallel lamellar structure. Well-ordered lamellae are recovered in this "dry-spray" limit, however, if a much lower molecular weight (unentangled) BCP is used, reflecting the expected molecular weight sensitivity of the relaxation kinetics.

These results elucidate the particular importance of residual solvent content and molecular weight in dictating the morphology developed during electrospray deposition. It is apparent that electrospray offers a unique platform that enables the combination of thermal and solvent annealing effects in situ during continuous deposition of block copolymers and as such it is a versatile tool for BCP thin film processing.

ASSOCIATED CONTENT

Supporting Information

SEM and optical microscope images of PS-*b*-P4VP (20K−17K). This material is available free of charge via the Internet at http://pubs.acs.org.

AUTHOR INFORMATION

Corresponding Author

*E-mail: chinedum.osuji@yale.edu.

Notes

The authors declare no competing financial interest.

ACKNOWLEDGMENTS

The authors gratefully acknowledge funding support from NSF (DMR-0847534; CMMI-1246804). H.H. and J.P.S. acknowledge additional financial support from ONR YIP award N000141210657. C.O. acknowledges additional financial support from 3M Nontenured Faculty Award. Facilities use was supported by YINQE and NSF MRSEC DMR-1119826.

REFERENCES

(1) Park, M.; Harrison, C.; Chaikin, P. M.; Register, R. A.; Adamson, D. H. *Science* **1997**, *276* (5317), 1401−1404.
(2) Ruiz, R.; Kang, H. M.; Detcheverry, F. A.; Dobisz, E.; Kercher, D. S.; Albrecht, T. R.; de Pablo, J. J.; Nealey, P. F. *Science* **2008**, *321* (5891), 936−939.
(3) Tang, C. B.; Lennon, E. M.; Fredrickson, G. H.; Kramer, E. J.; Hawker, C. J. *Science* **2008**, *322* (5900), 429−432.
(4) Lee, J. I.; Cho, S. H.; Park, S. M.; Kim, J. K.; Kim, J. K.; Yu, J. W.; Kim, Y. C.; Russell, T. P. *Nano Lett.* **2008**, *8* (8), 2315−2320.
(5) Cheng, J. Y.; Ross, C. A.; Chan, V. Z. H.; Thomas, E. L.; Lammertink, R. G. H.; Vancso, G. J. *Adv. Mater.* **2001**, *13* (15), 1174−1178.
(6) Thurn-Albrecht, T.; Schotter, J.; Kastle, C. A.; Emley, N.; Shibauchi, T.; Krusin-Elbaum, L.; Guarini, K.; Black, C. T.; Tuominen, M. T.; Russell, T. P. *Science* **2000**, *290* (5499), 2126−2129.
(7) Urbas, A.; Sharp, R.; Fink, Y.; Thomas, E. L.; Xenidou, M.; Fetters, L. J. *Adv. Mater.* **2000**, *12* (11), 812−814.
(8) Urbas, A. M.; Maldovan, M.; DeRege, P.; Thomas, E. L. *Adv. Mater.* **2002**, *14* (24), 1850−1853.
(9) Fink, Y.; Urbas, A. M.; Bawendi, M. G.; Joannopoulos, J. D.; Thomas, E. L. *J. Lightwave Technol.* **1999**, *17* (11), 1963−1969.
(10) Yang, S. Y.; Ryu, I.; Kim, H. Y.; Kim, J. K.; Jang, S. K.; Russell, T. P. *Adv. Mater.* **2006**, *18* (6), 709−712.
(11) Yang, S. Y.; Park, J.; Yoon, J.; Ree, M.; Jang, S. K.; Kim, J. K. *Adv. Funct. Mater.* **2008**, *18* (9), 1371−1377.
(12) Phillip, W. A.; O'Neill, B.; Rodwogin, M.; Hillmyer, M. A.; Cussler, E. L. *ACS Appl. Mater. Interfaces* **2010**, *2* (3), 847−853.
(13) Elabd, Y. A.; Hickner, M. A. *Macromolecules* **2011**, *44* (1), 1−11.

(14) Zhang, Q. L.; Cirpan, A.; Russell, T. P.; Emrick, T. *Macromolecules* **2009**, *42* (4), 1079−1082.
(15) Crossland, E. J. W.; Nedelcu, M.; Ducati, C.; Ludwigs, S.; Hillmyer, M. A.; Steiner, U.; Snaith, H. J. *Nano Lett.* **2009**, *9* (8), 2813−2819.
(16) Hu, H.; Gopinadhan, M.; Osuji, C. O. *Soft Matter* **2014**, *10*, 3867−3889.
(17) Han, E.; Stuen, K. O.; La, Y. H.; Nealey, P. F.; Gopalan, P. *Macromolecules* **2008**, *41* (23), 9090−9097.
(18) Kim, S.; Bates, C. M.; Thio, A.; Cushen, J. D.; Ellison, C. J.; Willson, C. G.; Bates, F. S. *ACS Nano* **2013**, *7* (11), 9905−9919.
(19) Kim, S. H.; Misner, M. J.; Xu, T.; Kimura, M.; Russell, T. P. *Adv. Mater.* **2004**, *16* (3), 226−231.
(20) Knoll, A.; Horvat, A.; Lyakhova, K. S.; Krausch, G.; Sevink, G. J. A.; Zvelindovsky, A. V.; Magerle, R. *Phys. Rev. Lett.* **2002**, *89*, 035501.
(21) Fukunaga, K.; Elbs, H.; Magerle, R.; Krausch, G. *Macromolecules* **2000**, *33* (3), 947−953.
(22) Keller, A.; Pedemont, E.; Willmout, Fm. *Nature* **1970**, *225* (2), 538−539.
(23) Chen, Z. R.; Kornfield, J. A.; Smith, S. D.; Grothaus, J. T.; Satkowski, M. M. *Science* **1997**, *277* (5330), 1248−1253.
(24) Boker, A.; Elbs, H.; Hansel, H.; Knoll, A.; Ludwigs, S.; Zettl, H.; Zvelindovsky, A. V.; Sevink, G. J. A.; Urban, V.; Abetz, V.; Muller, A. H. E.; Krausch, G. *Macromolecules* **2003**, *36* (21), 8078−8087.
(25) Gopinadhan, M.; Majewski, P. W.; Osuji, C. O. *Macromolecules* **2010**, *43* (7), 3286−3293.
(26) Gopinadhan, M.; Majewski, P. W.; Choo, Y.; Osuji, C. O. *Phys. Rev. Lett.* **2013**, *110*, 078301.
(27) Angelescu, D. E.; Waller, J. H.; Adamson, D. H.; Deshpande, P.; Chou, S. Y.; Register, R. A.; Chaikin, P. M. *Adv. Mater.* **2004**, *16* (19), 1736−1740.
(28) Angelescu, D. E.; Waller, J. H.; Register, R. A.; Chaikin, P. M. *Adv. Mater.* **2005**, *17* (15), 1878−1881.
(29) Yager, K. G.; Fredin, N. J.; Zhang, X.; Berry, B. C.; Karim, A.; Jones, R. L. *Soft Matter* **2010**, *6* (1), 92−99.
(30) Berry, B. C.; Bosse, A. W.; Douglas, J. F.; Jones, R. L.; Karim, A. *Nano Lett.* **2007**, *7* (9), 2789−2794.
(31) Hashimoto, T.; Bodycomb, J.; Funaki, Y.; Kimishima, K. *Macromolecules* **1999**, *32* (3), 952−954.
(32) Singh, G.; Batra, S.; Zhang, R.; Yuan, H.; Yager, K. G.; Cakmak, M.; Berry, B.; Karim, A. *ACS Nano* **2013**, *7* (6), 5291−9.
(33) Singh, G.; Yager, K. G.; Berry, B.; Kim, H.-C.; Karim, A. *ACS Nano* **2012**, *6* (11), 10335−10342.
(34) Tang, C. B.; Tracz, A.; Kruk, M.; Zhang, R.; Smilgies, D. M.; Matyjaszewski, K.; Kowalewski, T. *J. Am. Chem. Soc.* **2005**, *127* (19), 6918−6919.
(35) Tang, C. B.; Wu, W.; Smilgies, D. M.; Matyjaszewski, K.; Kowalewski, T. *J. Am. Chem. Soc.* **2011**, *133* (30), 11802−11809.
(36) Hu, H.; Rangou, S.; Kim, M.; Gopalan, P.; Filiz, V.; Avgeropoulos, A.; Osuji, C. O. *ACS Nano* **2013**, *7* (4), 2960−70.
(37) Ganan-Calvo, A. M.; Davila, J.; Barrero, A. *J. Aerosol Sci.* **1997**, *28* (2), 249−275.
(38) Barton, A. F. M. *CRC Handbook of Solubility Parameters and Other Cohesion Parameters*, 2nd ed.; CRC Press: Boca Raton, FL, 1991.
(39) Lide, D. R. *Handbook of Organic Solvents*. CRC Press: Boca Raton, FL, 1994.
(40) Haynes, W. M. *CRC Handbook of Chemistry and Physics*; CRC Press: Boca Raton, FL, 2012.
(41) Barton, A. F. M. *CRC Handbook of Polymer−Liquid Interaction Parameters and Solubility Parameters*; CRC Press: Boca Raton, FL, 1990.
(42) O'Driscoll, S.; Demirel, G.; Farrell, R. A.; Fitzgerald, T. G.; O'Mahony, C.; Holmes, J. D.; Morris, M. A. *Polym. Adv. Technol.* **2011**, *22* (6), 915−923.
(43) de Gennes, P. G. *Eur. Phys. J. E* **2001**, *6* (5), 421−424.
(44) Okuzono, T.; Ozawa, K.; Doi, M. *Phys. Rev. Lett.* **2006**, *97* (13), 136103.
(45) Gotrik, K. W.; Ross, C. A. *Nano Lett.* **2013**, *13* (11), 5117−5122.
(46) Zhang, X. J.; Harris, K. D.; Wu, N. L. Y.; Murphy, J. N.; Buriak, J. M. *ACS Nano* **2010**, *4* (11), 7021−7029.
(47) Borah, D.; Shaw, M. T.; Holmes, J. D.; Morris, M. A. *ACS Appl. Mater. Interfaces* **2013**, *5* (6), 2004−2012.
(48) Gennes, P. G. d. *J. Chem. Phys.* **1971**, *55* (2), 572.
(49) Fetters, L. J.; Lohse, D. J.; Richter, D.; Witten, T. A.; Zirkel, A. *Macromolecules* **1994**, *27* (17), 4639−4647.